Deterministic Microfluidic Ratchet

Kevin Loutherback,[1,2] Jason Puchalla,[3] Robert H. Austin,[1,3] and James C. Sturm[1,2]

[1]*Princeton Institute for Science and Technology of Materials (PRISM), Princeton, New Jersey, USA*
[2]*Department of Electrical Engineering, Princeton University, Princeton, New Jersey, USA*
[3]*Department of Physics, Princeton University, Princeton, New Jersey, USA*

(Received 18 August 2008; revised manuscript received 27 October 2008; published 26 January 2009)

We present a deterministic, nonthermal ratchet where the trajectory of particles in a certain size range is not reversible when the sign of the pressure gradient is reversed at a low Reynolds number. This effect is produced by employing triangular rather than the conventional circular posts in an array that selectively displaces particles transported through the array. The ratchet irreversibly moves particles of a certain size range in a direction orthogonal to an oscillating flow, with no net displacement of the fluid itself. The underlying mechanism of this ratchet is shown to be connected to irreversible particle-post interactions and the asymmetric fluid velocity distribution through the gap between the triangular posts. Diffusion plays no role in this ratchet, and hence the device parameters presented here can be scaled up to high rates of flow, of clear importance in separation technologies.

DOI: 10.1103/PhysRevLett.102.045301 PACS numbers: 05.60.Cd, 05.20.Dd

A deterministic microfluidic ratchet for particles within a certain size range is presented in this Letter. Numerous schemes for separating particles using Brownian motion in a ratchet have been demonstrated [1–5]. However, the rate of separation in these methods is limited by target particles' rate of diffusion while the weak dependence of the diffusion constant on particle size further limits resolution. Microfluidic devices usually operate at low Reynolds number [6–8]. In this regime, the fluid flow through an arbitrary geometry can be considered to be time invariant—reversing the applied pressure gradient will reverse the flow field because inertial effects are negligible [9]:

$$\eta \nabla^2 \vec{v} = -\nabla P, \tag{1}$$

where η is the viscosity of the fluid. Reversal of the sign of the pressure gradient $-\nabla P$ reverses the fluid velocity $\vec{v}$. Thus in the absence of diffusion and any external forces particle motion is also time reversible. However irreversible forces exist in our system in the form of steric repulsion between particles suspended in the fluid and posts that obstruct the fluid flow [10]. When a particle in the fluid runs into a post, it is displaced from its initial streamline to an adjacent streamline. As shown in Fig. 1, if the fluid flow is reversed, it will not return to its original position, but rather travel back along its new streamline unless it is displaced by some other obstacle. This motion by particles across streamlines due to contact forces makes particle movement in the presence of obstacles irreversible in time and critical to the effect we will describe in this Letter. Note that the irreversible change in direction occurs as the particle moves through the gap on the return pass, not the turning point of the motion as the flow is reversed. This phenomenon of motion across streamlines has been employed in microfabricated post arrays for continuous-flow separation of particles over a large operating range (100 nm to 30 μm) [11,12] for a variety of objects including polystyrene beads, DNA [13], bacteria [14], and human blood cells [11,15–17], with a resolving power down to 10 nm [13].

A micrograph of a device (''ratchet bump array'') which demonstrates nonthermal ratcheting with flow reversal is shown in Fig. 2. This array consists of a lattice of right triangular posts that is rotated at angle ϵ with respect to the average fluid flow direction. The results of this Letter are presented using an array with pitch of 10 μm and a tilt angle ϵ of 5.71° (0.1 rad). Right isosceles triangular posts with 6 μm leg length were used, giving a gap G between posts of approximately 4 μm. The array was microfabricated in silicon by reactive-ion etching to a depth of

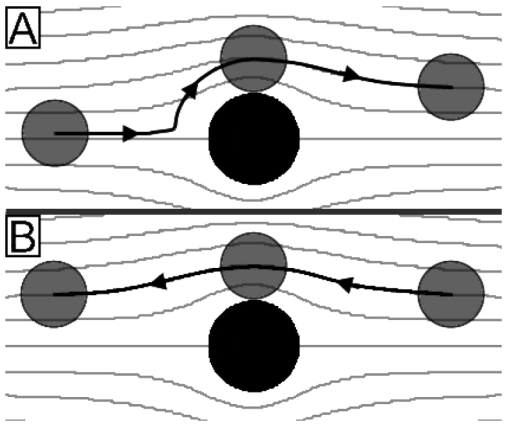

FIG. 1. Irreversible particle motion results when a particle runs into an obstacle. (a) A particle moving left to right is displaced to a new streamline when it runs into a post. (b) When the flow is reversed, the particle does not cross a streamline but instead follows its new streamline and returns to a different initial position.

 © 2009 The American Physical Society

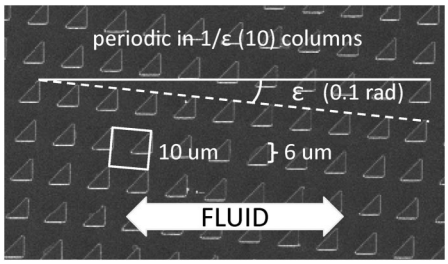

FIG. 2. Micrograph of the ratcheting triangular post array used in the experiments presented here. The right isosceles triangles are 6 μm on a side with post-to-post separation of 10 μm and tilt angle of 5.71° (0.1 rad) with respect to the fluid flow. Confining walls on the top and bottom of the device (not shown) force the fluid to flow on average horizontally. The solid line represents the fluid flow direction and the dotted line represents the post array rotation.

approximately 10 μm and then sealed with a polydimethysiloxane (PDMS)-coated glass slide. The fluid was driven by applied pressure of a hand-operated syringe pump and observed with epifluorescent microscopy.

We observe a highly unusual ratcheting motion in an array of triangular posts oriented as shown in Fig. 2. The behavior of large and small particles in this array qualitatively matches with that previously observed in arrays with circular posts. Particles smaller than some critical size travel in the average direction of fluid flow and show no orthogonal displacement after the flow direction is cycled multiple times. Larger particles are displaced (''bumped'') at each column of posts and move at an angle ϵ with respect to the average fluid flow [13] but return to their original position after one flow cycle. This behavior is shown in the time-lapse images of the motion of small (1.1 μm) and large (3.1 μm) fluorescent polystyrene beads when the fluid flow direction was reversed multiple times [Figs. 3(a) and 3(b)]. (The Reynolds number is $\sim 10^{-3}$ for approximate fluid velocities $\sim$250 μm/s and characteristic length (gap) $\sim$4 μm.)

However, we observed a third possible behavior only in the array with triangular posts: particles with an intermediate size (1.9 μm) did not retrace their trajectory when the fluid flow was reversed—rather, they followed the trajectory of large particles moving right to left and approximately that of small particles when moving left to right [Fig. 3(c)]. When the fluid flow was cycled back and forth, the net motion of these particles was roughly perpendicular to the axis of fluid motion, leaving the particles displaced vertically from their original surrounding plug of fluid without any net motion of the fluid. After many cycles, the particles were concentrated along the upper edge of the device in spite of the zero net fluid displacement.

To understand the irreversibility of this ratchet effect, first consider the fluid flow in showing an array with $\epsilon = 1/3$ at zero Reynolds number [18] [see Fig. 4(a)]. The bump array relies on the asymmetric bifurcation of fluid

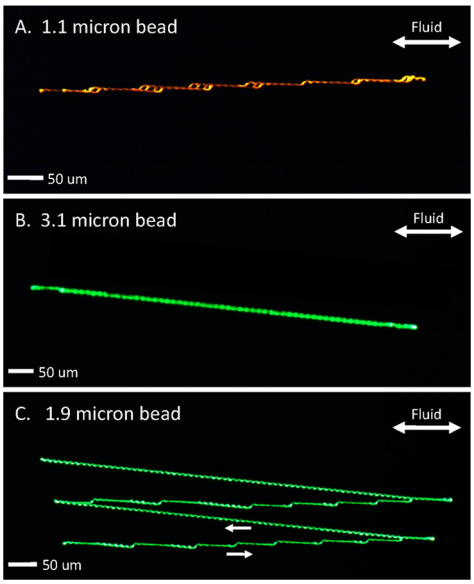

FIG. 3 (color online). Time-lapse image of the trajectories of spherical polystyrene beads in a triangular post array oriented as in Fig. 2 as the direction of fluid flow is cycled back and forth twice. Particle diameters are (a) 1.1 μm, (b) 3.1 μm, and (c) 1.9 μm. Particles in (a) and (b) retrace their paths when the direction of the fluid is reversed, while the trajectory in (c) changes with the direction of the fluid flow. In (c), small arrows indicate the direction of the fluid along the particle path.

streams around the posts due to the array rotation: fluid stream tubes flowing through a gap are split around a post in the next column, with $1 - \epsilon$ of the fluid going through the next gap while the other ϵ of fluid goes around the other side of the next post. As a result, the fluid motion can be characterized by $1/\epsilon$ stream tubes of equal volume flow (three in the case of Fig. 4) that cycle through positions in the gap, but travel horizontally on average. The stagnation streamlines shown in Fig. 4 act as the boundaries between the three stream tubes and denote how the fluid will divide around posts.

The pivotal location for determining particle trajectories in the array is the gap between two posts G, where the stream tubes are narrowest. Consider particles traveling left to right in the stream tube just above the post. If a particle suspended in the fluid is small compared to the width W_c or W_{tri} of the stream tube closest to the post, it will stay in the stream tube and travel in the average fluid flow direction. If the particle is large enough, it will be displaced across a stagnation streamline by the post into the next stream tube. For a hard sphere, the critical size for such a displacement occurs when the particle radius is equal to the width of the stream tube adjacent to the post. Since the new stream tube becomes the one adjacent to the post in the next column of the post, large particles are locked into being ''bumped'' into an adjacent stream tube at every column and the particle will travel along the array clear axis instead of horizontally with the fluid and small

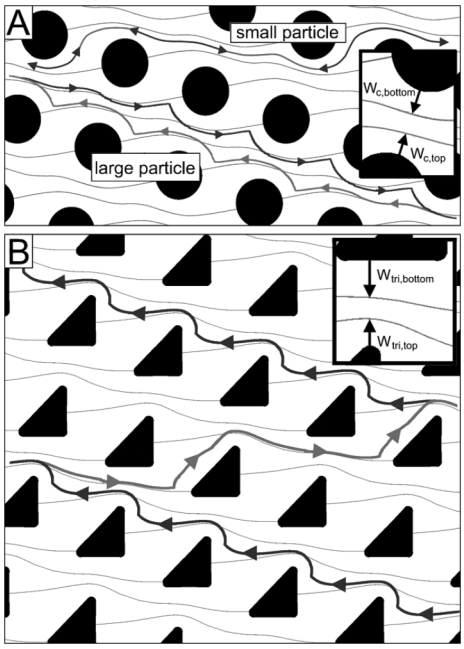

FIG. 4. Schematic of flow in post arrays with ϵ of $1/3$, showing boundaries between three stream tubes of equal flow between each gap for (a) round posts and (b) triangular posts. Insets indicate the widths of the stream tubes in the gap adjacent to the posts in each cases. Shown in (a) is the path of a ''small'' and a ''large'' particle moving left to right and then right to left, both sizes return to the same position with one cycle. Shown in (b) is the path of a ratcheting particle in a triangular post array, where it acts as a large particle traveling right to left but as a small particle when traveling left to right, resulting in a net vertical displacement after 1.5 cycles of pressure.

particles, but with no net displacement after one pressure cycle.

This is not true for a rotated array of right triangular posts as seen in Fig. 4(b). As in the circular posts of Fig. 4(a), small particles are not displaced by the posts and retrace their trajectory if the flow is reversed; there is no net displacement. Large particles are irreversibly displaced at each column of posts, but note that the large particle in Fig. 3(a) is displaced by the lower edges of the posts when moving left to right and by the upper edges of obstacles when moving right to left. Intermediate size particles move in stream tubes nearest the sharp vertex of the triangle post when moving right to left, and in the stream tube nearest the flat triangle side when moving left to right as is shown in Fig. 4(c). Thus, the ratcheting characteristic of an array of triangular posts is a result of breaking spatial symmetry of the width of the stream tubes by the triangle posts within the gap G.

Because of the top-bottom symmetry of circular posts, the width W_{circ} of the stream tubes closest to the circular posts on either side of the gap is identical:

$$W_{\mathrm{circ,top}} = W_{\mathrm{circ,bottom}}. \tag{2}$$

For triangular posts, the velocity of flow is highest at the triangle vertex and hence the stream tubes are smallest there. Qualitatively, the width of the first stream tube W_{tri} above the triangular post (near the upper vertex of the triangle) is narrower than that of the first stream tube below the post (near the horizontal edge of the triangle):

$$W_{\mathrm{tri,top}} > W_{\mathrm{tri,bottom}}. \tag{3}$$

As a result, the critical size for particles moving left to right can be smaller than that for particles moving right to left depending on the particle's size. If a particle falls in between the two critical sizes, it acts like a ''small'' particle when moving left to right and like a ''large'' particle when moving right to left. This leads to a ratcheting behavior and is what is observed with the intermediate-sized bead in Fig. 3(c).

To quantify the difference in critical particle size between the vertex and the flat side of the triangular posts, we employed the method Inglis *et al.* [19] used to determine the critical particle size in a circular post array. To find the width of the first stream tube adjacent to a post, we integrate over the velocity profile from either edge of the gap until the flux equals ϵ times the total flux through a gap. This is represented symbolically as

$$\epsilon \int_0^G u(s)ds = \int_0^{R_v} u(s)ds = \int_{R_f}^G u(s)ds, \tag{4}$$

where R_v is the critical particle radius near the vertex, R_f is the critical particle radius near the flat, and $u(s)$ is the total velocity as a function of position in the gap. The velocity profiles were found to be independent of the tilt angle ϵ over a large range of tilt angles (between $1/2$ and $1/100$ rad) so the flow profiles in Fig. 5 can be used as $u(s)$ for any array tilt in this range. Fluid in streams adjacent to the posts have been shaded in Fig. 4 for the case of $\epsilon = 1/3$ to demonstrate the shift of flux towards the vertex. The width of these streams are $0.34G$ for the triangle vertex, $0.42G$ for the triangle flat, and $0.39G$ for both edges of the circular posts.

Using this method, we can predict what size particles will show ratcheting behavior. Figure 6 shows the calculated critical diameter as a ratio of the gap for the vertex and flat of the triangle versus array tilt angle (with no adjustable parameters). The observed data points of Fig. 3 for $\epsilon = 1/10$ are plotted as crosses. There is excellent agreement between the observed modes of the three particle sizes and prediction. The 1.1 μm ($0.24G$) bead is smaller than both critical particle sizes so it travels with the fluid in both directions and shows no net displacement when the fluid direction is cycled. The 3.1 μm ($0.66G$) particle is bigger than both critical particle sizes so it is displaced along the array axis in both directions and shows no net displacement when the fluid direction is cycled. The 1.9 μm ($0.41G$) particle is in between the two critical particle sizes so it travels with the fluid when it moves

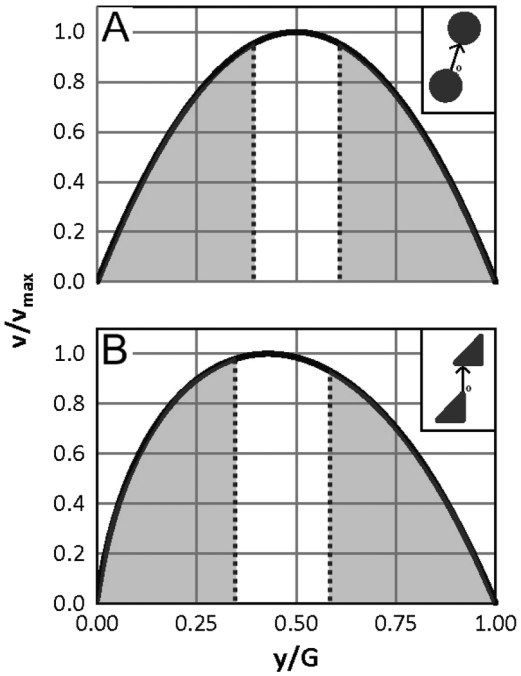

FIG. 5. Normalized velocity profile across gaps with (a) round and (b) triangular posts. Insets shows orientation of cross-sectional line. Shaded areas bound by dotted lines indicate fluid in stream tubes closest to a post on either side of the gap for $\epsilon = 1/3$.

along the flat edge of the triangle and with the array axis when it moves along the vertex of the triangle.

In summary, we have shown that a deterministic ratchet can be constructed by using triangular rather than circular posts in a microfabricated post array. By combining the irreversible interaction of a particle being displaced by an obstacle in the fluid and the broken symmetry that results from using triangular posts, we are able to separate select particles orthogonal to the fluid flow. In contrast to Brownian ratchets, which must be operated ''slowly'' to allow for diffusion, the device presented here in principal would operate effectively at higher speeds because of its deterministic nature. Thus the principles in this Letter may lead to a new class of ratchet devices which could be useful for technological application.

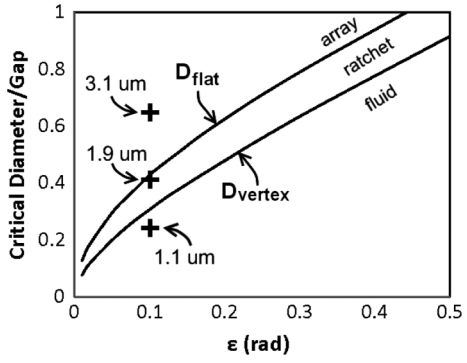

FIG. 6. Predicted critical diameter as a ratio of gap for flat edge and triangle vertex versus array tilt angle. Central shaded region indicates range of particles that will exhibit ratcheting behavior under oscillatory flow. Experimental results for $\epsilon = 1/10$ indicated by ''+'' for 3.1 μm (0.66G), 1.9 μm (0.41G), and 1.1 μm (0.24G) beads.

This work was supported by the AFOSR (FA9550-05-01-0365), NIH (HG01506), NSF Cornell Nanobiology Technology Center (BSC-ECS9876771), and DARPA. We thank William Russel at Princeton for helpful discussions, Keith Morton for etching of the devices, Steve Chou for use of his etching facility, and we particularly thank the referees for their constructive comments.

[1] S. Matthias and F. Muller, Nature (London) **424**, 53 (2003).
[2] I. Derenyi and R. D. Astumian, Phys. Rev. E **58**, 7781 (1998).
[3] C. Marquet *et al.*, Phys. Rev. Lett. **88**, 168301 (2002).
[4] M. Caboti *et al.*, Electrophoresis **23**, 1046 (2002).
[5] A. van Oudenaarden *et al.*, Science **285**, 1046 (1999).
[6] T. M. Squires and S. R. Quake, Rev. Mod. Phys. **77**, 977 (2005).
[7] H. A. Stone, A. D. Stroock, and A. Ajdari, Annu. Rev. Fluid Mech. **36**, 381 (2004).
[8] D. Erickson and D. Q. Li, Anal. Chim. Acta **507**, 11 (2004).
[9] R. P. Feynman, R. B. Leighton, and M. Sands, *The Feynman Lectures on Physics* (Addison-Wesley, Reading, MA, 1966).
[10] P. M. Chaikin and T. C. Lubensky, *Principles of Condensed Matter Physics* (Cambridge University Press, Cambridge, England, 1995).
[11] J. A. Davis *et al.*, Proc. Natl. Acad. Sci. U.S.A. **103**, 14 779 (2006).
[12] K. J. Morton, J. C. Sturm, R. H. Austin, and S. Y. Chou, in *Proceedings of the Micro Total Analysis Systems Conference 2006, Tokyo* (Chemical and Biological Microsystems Society, San Diego, 2006), pp. 1014–1016.
[13] L. R. Huang, E. C. Cox, R. H. Austin, and J. C. Sturm, Science **304**, 987 (2004).
[14] K. J. Morton *et al.*, Lab Chip **8**, 1448 (2008).
[15] D. W. Inglis *et al.*, Lab Chip **8**, 925 (2008).
[16] D. W. Inglis *et al.*, J. Immunol. Methods **329**, 151 (2008).
[17] K. J. Morton *et al.*, Proc. Natl. Acad. Sci. U.S.A. **105**, 7434 (2008).
[18] Velocity fields for array geometries like that shown in Fig. 4 were modeled by solution of the 2D incompressible Navier-Stokes equation in finite-element solver COMSOL Multiphysics 3.4, and the velocity profile across a heavily meshed gap was extracted for analysis. Triangle vertices were rounded with a curvature of 500 nm to approximate the vertex roundness produced by photolithographic methods.
[19] D. W. Inglis, J. A. Davis, R. H. Austin, and J. C. Sturm, Lab Chip **6**, 655 (2006).